

RESEARCH ARTICLE

Monitoring Response to Radiotherapy in Human Squamous Cell Cancer Bearing Nude Mice: Comparison of 2'-deoxy-2'-[¹⁸F]fluoro-D-glucose (FDG) and 3'-[¹⁸F]fluoro-3'-deoxythymidine (FLT)

Carla F. M. Molthoff,¹ Bianca M. Klabbers,² Johannes Berkhof,³ Jasper T. Felten,¹ Marcelle van Gelder,¹ Albert D. Windhorst,¹ Ben J. Slotman,² Adriaan A. Lammertsma¹

¹Department of Nuclear Medicine and PET Research, VU University Medical Center, P.O. Box 7057, 1007, Amsterdam, The Netherlands

²Department of Radiotherapy, VU University Medical Center, Amsterdam, The Netherlands

³Department of Epidemiology and Biostatistics, VU University Medical Center, Amsterdam, The Netherlands

Abstract

Objective: The uptake of 3'-[¹⁸F]fluoro-3'-deoxythymidine (FLT), a proliferation marker, was measured before and during fractionated radiotherapy to evaluate the potential of FLT-positron emission tomography (PET) imaging as an indicator of tumor response compared to 2'-deoxy-2'-[¹⁸F]fluoro-D-glucose (FDG).

Materials and Methods: Nude mice bearing established human head and neck xenografts (HNX-OE; nu/nu mice) were locally irradiated (three fractions/week; 22 Gy) using a 150-kV_p unit. Multiple FDG- and FLT-PET scans were acquired during treatment. Tumor volume was determined regularly, and tissue was analyzed for biomarkers involved in tracer uptake.

Results: Both groups revealed a significant decline in tumor volume ($P < 0.01$) compared to untreated tumors. For FDG as well as for FLT, a significant decline in retention was observed at day 4. For FLT, most significant decline in retention was observed at day 12; whereas, for FDG, this was already noted at day 4. Maximum decline in tumor-to-nontumor ratios (T/NT) for FDG and FLT was $42 \pm 18\%$ and $49 \pm 16\%$ (mean \pm SD), respectively. FLT uptake was higher than that of FDG. For FLT, statistical significant correlations were found for both tumor volume at baseline and at day 29 with T/NT and Δ T/NT. All tumors demonstrated expression of glucose transporter-1, thymidine kinase-1, and hexokinase II. No differences were found for amount of tumor cells and necrosis at the end of treatment.

Conclusion: This new experimental *in vivo* model supports the promise of using FLT-PET, as with FDG-PET, to monitor response to external radiotherapy. This warrants further clinical studies to compare these two tracers especially in cancers treated with radiotherapy.

Key words: FDG, FLT, PET, Radiotherapy, Response monitoring, Head and neck xenograft model

Introduction

Head and neck cancer represents 5% of all malignancies diagnosed annually, and >90% of tumors are of the

squamous cell type [1]. The overall 5-year survival rate for patients with head and neck squamous cell carcinoma (HNSCC) of 50% is among the lowest of the major cancer types [2]. Traditional staging of HNSCC depends on site of disease, size and extent of the primary tumor, cervical lymph node involvement, and presence or absence of distant metastasis [3]. Currently, surgery and radiotherapy are treatments of choice for primary HNSCC, with chemotherapy reserved for more widespread disease [4]. Because of variations in biological behavior, tumors of the same stage often respond differently to the same treatment. Therefore, not only correct staging of HNSCC but also monitoring response to treatment is essential.

Unlike computed tomography and magnetic resonance imaging, which are anatomical imaging techniques, positron emission tomography (PET) is a quantitative molecular imaging modality that allows for noninvasive *in vivo* imaging and quantification of biological processes, such as metabolism, receptor density, cell proliferation, and uptake of therapeutic agents. Consequently, PET is a valuable tool for detecting and especially staging of various tumor types. 2'-deoxy-2'-[¹⁸F]fluoro-D-glucose (FDG), a glucose analog, is the most commonly used PET tracer in oncology, with diagnostic, staging, and response monitoring applications [5, 6]. A disadvantage of FDG-PET is uptake in other tissues with physiologically high glucose consumption, such as brain, muscle, inflammatory tissue, macrophages, and lymphocytes [7]. In addition, FDG is less suitable for monitoring response after/during radiotherapy, as often increased uptake is seen after radiation caused by inflammatory lesions and fibrosis [8–11].

Therefore, other tracers have been developed, such as 3'-[¹⁸F]fluoro-3'-deoxythymidine (FLT), which is considered to be more specific for proliferation, another characteristic of tumor cells [12–14]. FLT is retained in proliferating tissues after it is phosphorylated by cytosolic thymidine kinase-1 (TK-1), one of the key cytosolic enzymes in the synthesis of DNA [15–19]. In most species, no metabolites of FLT can be demonstrated [12]; only in monkeys and humans glucuronidation of FLT has been observed. Shields et al. [13] have demonstrated that it is possible to image tumor cell proliferation using FLT. In general, sensitivity of detecting tumors by FLT is comparable to that with FDG [12, 20]. Detection of bone metastases is more difficult with FLT because of high physiological uptake of FLT in proliferating bone marrow cells. However, unlike FDG, FLT is able to discriminate between tumor and inflammatory tissue [21]. Therefore, FLT might be a suitable marker for tumor response monitoring, especially after radiation therapy.

In the present study, first radiosensitivity of the human head and neck cancer xenograft HNX-OE [22, 23] was investigated. Next, FDG and FLT uptake in tumors during and after fractionated radiotherapy was investigated within the context of monitoring response to therapy. *In vivo* tracer uptake was correlated with efficacy of radiotherapy and with biological features in excised tumors subsequently.

Materials and Methods

Animal Model

Both flanks of NMRI nu/nu mice (age, 8–10 weeks; weight, 22–28 g; Harlan, Zeist, the Netherlands) were implanted subcutaneously with small tissue pieces of the human HNSCC HNX-OE, as described previously [24]. Mice were kept in sterile surroundings with standardized light/dark cycle and access to food and water ad libitum. Tumor size was determined by caliper measurements at least twice a week using the formula $T_{vol} = \frac{l \cdot w \cdot h}{2}$ (l , length; w , width; h , height of the tumor) [25, 26]. Treatment started at tumor volumes between 50 and 150 mm³. After the experiment, mice were sacrificed and tumor tissue was rapidly excised. Tumors were excised at days 38 and 36 after start of treatment for the FDG and FLT group, respectively. Mice from the control group were killed at day 16. All animal experiments were carried out in accordance with the Dutch Law on Animal Experimentation and the institutional committee on animal experimentation.

Radiotherapy

Local external beam radiation was applied using a clinical X-ray therapy unit (PANTAK Therapax SXT, 150 kV photon, filter 8 [0.2 Al+1.0 Cu]) at a dose rate of 206.6 Gy/min. For homogeneous dose distributions, anteroposterior and posteroanterior external beam radiotherapy fields were used. Radiation was performed under intraperitoneally anesthesia using a mixture of Ketamine/xylazine (2/1; 1 ml/kg; i.p.).

Experimental Design

Radiosensitivity As radiosensitivity of the tumor line HNX-OE was unknown, a maximum tolerated dose (MTD) finding study was carried out first. MTD is defined as a weight loss of maximally 10% in the group of mice, with a maximum of 15% per individual mouse. The weight of the mice was measured three times a week. Tumor-bearing nude mice were randomized into five groups of six mice each. Xenografts were exposed locally to a single radiation dose of 10, 14, 18 or 22 Gy, while the fifth group was not irradiated (control group). Tumors were measured three times a week, and growth curves were established, relating mean volume over time to the volume on the first day of irradiation. Antitumor activity was expressed as tumor-to-control tumor volume ratio (T/C) in percentage to control. Increase in life span (ILS) was also calculated. ILS was defined as the median life span of the treated group divided by the median life span of the control group, using the day of transplantation as day 0. The day of death was defined as the day at which mice were taken off the experiment.

Differences in significance between the antitumor effects of a particular treatment were determined by means of Kaplan–Meier analysis.

Production of PET Tracers

FLT was produced according to the method described by Machulla et al. [27] with modifications. This procedure resulted in a good manufacturing practice (GMP) compliant, pyrogen-free, sterile production of FLT with a radiochemical purity >97% and an average (\pm SD) yield of 1.5 \pm 0.5 GBq and a mean specific activity

of 100.2 GBq/μmol. FDG was produced under GMP conditions for human use by BV Cyclotron VU (Amsterdam, the Netherlands) with a radiochemical purity of >97%.

PET Protocol

PET studies were performed with a double-LSO-layer High Resolution Research Tomograph (HRRT, CTI, Knoxville, TN), a dedicated animal and human brain scanner with no interplane septa (3D) and with depth-of-interaction information. This scanner combines high uniform spatial resolution with high absolute sensitivity [28]. For attenuation correction, a transmission scan using a single-photon 137-Cs transmission point source was acquired.

PET scans were acquired under inhalation anesthesia (mixture of 5% isoflurane: 95% oxygen). Acquisitions started 30 min after tracer injection. Data were acquired in list mode during 60 min and rebinned retrospectively into a series of four sinograms of 15 min duration. All data were normalized, corrected for attenuation, and reconstructed (using OSEM3D) into a series of image volumes with a cubical voxel size of 1.2 mm. Reconstructed resolution was almost isotropic with 2.2 mm full width at half maximum in the center of the field of view and 2.5 mm at 10 cm off-axis [28].

Response Monitoring Three groups, each of six tumor-bearing mice, were followed over time. One group served as control and the other two groups (FDG and FLT groups) were exposed to 22 Gy in six fractions over a 2-week treatment schedule. PET scans were performed in these latter two groups before and during radiotherapeutic treatment, according to the schedule depicted in Table 1. Tracer dose was 5.0±0.8 and 3.7±0.9 MBq for FDG and FLT, respectively.

PET Analysis

Three-dimensional (3-D) regions of interest (ROIs) were placed semiautomatically using dedicated software [29]. The tumor hot spot was interactively set in the plane where the tumor was best visible (frames 30–60 min), and ROIs were then set automatically using a 3-D region-growing algorithm around the tumor area and in a corresponding normal tissue next to the tumor area in all planes where the tumor was found. Tumor ROIs were copied to normal tissue to obtain normal tissue ROIs of comparable size and shape. Activity was calculated in pixels with an intensity of 70% compared to the most intense pixel. Reference ROIs were used for T/NT ratio calculation.

$$T/NT = \frac{\text{Radioactivity Concentration in Tumor (MBq/cc)}}{\text{Radioactivity Concentration in Normal Tissue (MBq/cc)}}$$

Table 1. Schematic outline of response monitoring experiment

Day	1	2	3	4	5	6	7	8	9	10	11	12	13	14	15
FDG group	A.M.	FDG	RTH		FDG				FDG	RTH		FDG			FDG
	P.M.	RTH		RTH				RTH	RTH		RTH				
FLT group	A.M.	FLT			FLT			FLT				FLT			
	P.M.	RTH	RTH		RTH	RTH		RTH				RTH			

RTH Radiotherapy fraction; FDG FDG PET scan; FLT FLT PET scan

Immunohistochemistry

Immunohistochemistry was performed on 4-μm thick formalin-fixed, paraffin-embedded or 5 μm of cryostat xenograft tissue sections as described earlier [30, 31]. Tumors were all excised at days 38 and 36 after start of treatment for the FDG and FLT group, respectively. Mice from the control group were all killed at day 16. Representative sections of tumors were quantitatively analyzed for the percentage of tumor cells, p53 nuclear staining and Ki67 expression, as described previously [30]. An experienced pathologist (G. M.), blinded to all other data, assessed the immunohistochemically stained slides on a multiheaded microscope in the presence of one junior (J. T. F.) and one senior (C. F. M. M.) researcher with experience in immunohistochemistry. The intensity of tumor cell cytoplasmic staining for vascular endothelial growth factor (VEGF) and hexokinase (HK) isoforms I, II, and III was graded as negative (–), weak (+), positive (2+), and strongly positive (3+), ignoring nuclear staining, which was frequently noted for all HKs. The numbers of cells with Glut-1 membrane and/or cytoplasmic staining, the amount of microvessels and CD68-positive macrophages, were semiquantitatively scored as none (–), occasionally (+), moderately frequent (2+), or frequent (3+).

Statistical Analysis

In the radiosensitivity study, treatment effects in each group were examined using Kaplan–Meier analysis (SPSS for Windows 11.0.1, SPSS, Chicago, IL) followed by a log-rank test.

In the response monitoring study, differences between control and FDG and FLT groups were examined by repeated measures analysis of variance followed by a least significant difference test. Univariate logistic regression was performed to assess the relation between tumor volume after radiotherapy and final PET values (T/NT). For testing associations between FDG and FLT accumulation (defined as low vs high) and biological markers (defined as negative/weak vs positive expression), a Fisher’s exact test was performed. Median values were used as cut-off levels. The strength of association between ordinal variables was represented by Spearman’s rank correlation.

Results

Radiosensitivity

To determine the radiosensitivity of human HNX-OE xenografts, tumors were locally irradiated with escalating doses of external beam radiation. Tumor growth in all treatment groups was inhibited compared with that in the control mice, in a dose-dependent way (Fig. 1). Tumor regrowth started 9 and 23 days after start of treatment in the

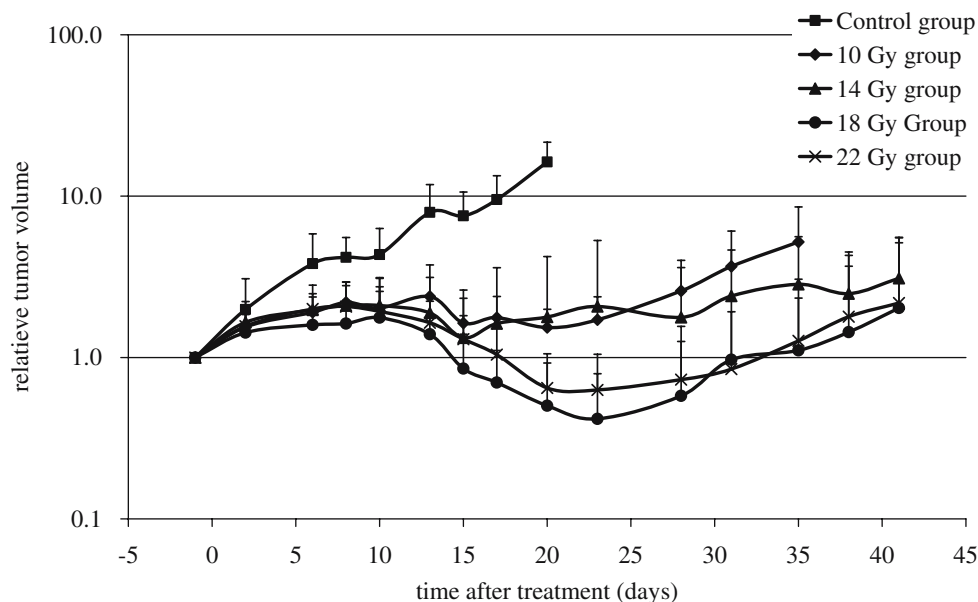


Fig. 1. Tumor growth of HNX-OE xenografts relative to tumor volume at start of local radiotherapy.

groups treated with 10 and 14 Gy and 18 and 22 Gy, respectively. A summary of treatment effects is listed in Table 2. All treated groups showed an ILS, and MTD was found to be 22 Gy. Statistical analysis demonstrated a significant difference ($P < 0.001$) between treated and control tumors. In addition, a significant difference was found between the 10 and 14 Gy group and the 18 and 22 Gy groups ($P < 0.007$).

No significant difference was found between tumors treated with doses of 18 and 22 Gy ($P = 0.379$).

Response Monitoring

Tumor-bearing mice received a baseline PET scan (FDG or FLT), and tumors were fractionated exposed to 22 Gy in total (six fractions, three times a week). Mice followed the schedule over 2 weeks, and results were compared with

tumor-bearing mice in the control group. The growth curve of HNX-OE tumor xenografts in untreated and irradiated mice is presented in Fig. 2. Statistical analysis demonstrated a significant difference ($P < 0.001$) between treated and control tumors from day 9 in both FDG and FLT group. No statistical significant difference was found between the FDG and FLT groups. A significant decline in tumor volume for FDG ($n = 12$ tumors) and FLT ($n = 11$ tumors) groups was found (both $P < 0.01$). For both groups, tumor regrowth started after day 29.

During radiotherapy, the maximum decline in T/NT measured for FDG and FLT was $42 \pm 18\%$ (scan 3) and $49 \pm 16\%$ (scan 4; mean \pm SD), respectively. At all time points, FLT uptake was higher than that for FDG, but FDG uptake showed less variation. For FLT, the decrease seen in the first week was followed by a much larger decrease in the second week (Fig. 3a, b). For FDG as well

Table 2. Treatment effects after radiotherapy of HNX-OE xenografts

Group	10 Gy	14 Gy	18 Gy	22 Gy
Irradiation dose ^a (Gy)	9.9 \pm 0.4	14.0 \pm 0.1	18.0 \pm 0.7	22.0 \pm 0.2
ILS ^b	188 \pm 99	336 \pm 127	420 \pm 112	413 \pm 192
T/C ^c				
Day 2	22 \pm 22	17 \pm 30	28 \pm 26	21 \pm 14
Day 6	50 \pm 13	48 \pm 23	58 \pm 12	48 \pm 13
Day 8	47 \pm 17	50 \pm 21	61 \pm 16	50 \pm 17
Day 10	50 \pm 11	57 \pm 30	68 \pm 20	56 \pm 19
Day 13	70 \pm 32	71 \pm 15	75 \pm 14	70 \pm 9
Day 15	77 \pm 10	82 \pm 17	88 \pm 7	82 \pm 8
Day 17	77 \pm 8	77 \pm 28	89 \pm 4	84 \pm 8
Day 20	81 \pm 22	81 \pm 19	94 \pm 4	91 \pm 4

^aDose in gray (Gy, mean \pm SD)

^bIncreased life span in percentage to control (mean \pm SD)

^cTumor-to-control tumor volume ratio (T/C) in percentage to control (mean \pm SD)

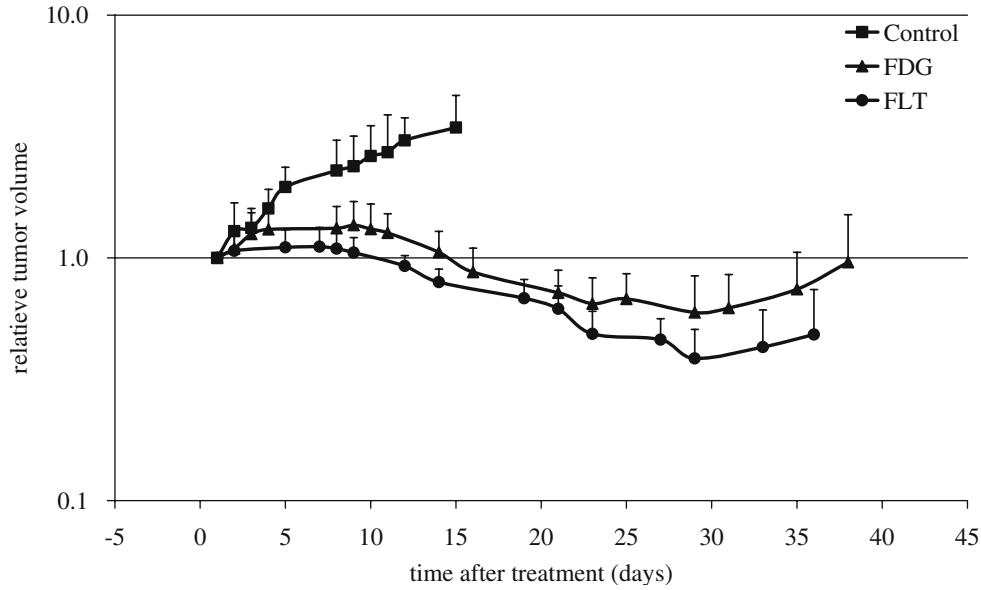


Fig. 2. Tumor growth of HNX-OE xenografts relative to tumor volume at start of local radiotherapy in controls and FDG and FLT groups.

as for FLT, a significant decline in retention (relative T/NT ratio) was observed at scan 2 (day 4). Next to this observation, for FLT, the most significant decline in retention (relative T/NT ratio) was observed at scan 4 (day 12), whereas for FDG, this was already noted from scan 2

(day 4). Table 3 summarizes the results from the statistical analyses correlating T/NT and changes in T/NT ($\Delta T/NT$) to tumor volumes at baseline ($V_{baseline}$) to exclude differences in the initial situation and at day 29 (V_{day29}). For FDG, no statistical significant correlation was found between $V_{baseline}$

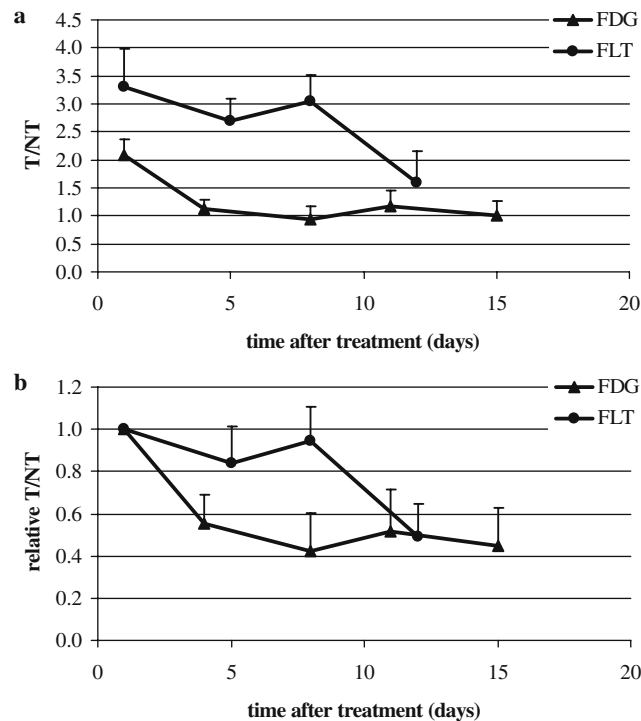


Fig. 3. FDG and FLT accumulation in HNX-OE xenografts. **a** absolute T/NT, tumor-to-nontumor ratio; **b** relative T/NT, tumor-to-nontumor ratio.

Table 3. Correlation between T/NT and tumor volume at baseline and at day 29 for FDG ($n=12$) and FLT ($n=11$)

	Tumor volume baseline (V_{baseline})		Relative tumor volume day 29 (V_{day29})	
	FDG	FLT	FDG	FLT
T/NT baseline	0.32	0.67 ^a	-0.67 ^a	-0.62 ^a
Delta T/NT 2 (scan 2—baseline)	-0.32	-0.62 ^a	0.57	0.65 ^a
Delta T/NT 3 (scan 3—baseline)	-0.48	-0.65 ^a	0.41	0.70 ^a
Delta T/NT 4 (scan 4—baseline)	-0.01	-0.17	0.30	0.51
Delta T/NT 5 (scan 5—baseline)	-0.10		0.14	

^aCorrelation is significant at the 0.05 level (two-tailed)

and any of the T/NT values. In contrast, for FLT, statistical significant correlations were found for both V_{baseline} and V_{day29} with T/NT and $\Delta T/NT$ of scans 2 and 3. Statistical significance disappeared with respect to scan 4 possibly because of the 4-day period between the last radiotherapy and scan 4. For FDG, only a significant correlation was found between V_{day29} and T/NT baseline. A predictive effect of baseline tumor volume was not found.

Immunohistochemistry

Table 4 summarizes the immunohistochemical results for irradiated tumors together with tumor cell density and amount of necrosis. Notable findings for irradiated tumors as compared to control tumors were high levels of Glut-1 expression (13 of 15 tumors), HK II (9 of 16 tumors), and Ki-67 expression (12 of 13 tumors). Expression of VEGF, HK I, HK III, and TK-1 expression was similar for control tumors and irradiated tumors. The same was true for number of tumor cells and necrosis. However, no statistical significant correlation could be demonstrated between the biomarkers at the end of treatment and FDG or FLT uptake. Histological findings showed severe radiation damage in tumors.

Discussion

In the present study, the PET tracers FDG and FLT were studied as potential tools for monitoring response during fractionated radiotherapy. In an animal model of head and neck cancer, the predictive value of FDG and FLT uptake for tumor response to radiotherapy was assessed. In

addition, tumor biology and radiosensitivity of these xenografts were studied.

To the best of our knowledge, there has been no report on the radiosensitivity of the human HNSCC HNX-OE xenografts. Knowledge of radiosensitivity is required to be able to use this animal model for radiation studies. Milas et al. [32] reported treatment of nu/nu mice bearing A431 tumor xenografts, derived from human epidermoid carcinoma, with a single dose of 18 Gy. Whether this dose equaled MTD was not reported. In a study of Jackel et al. [33] with hypopharynx carcinoma xenografts, radiation doses varied between 15 and 30 Gy, leading to a temporarily decrease in tumor volume. In the present model, using locally applied increasing radiation doses, MTD for HNX-OE xenografts was found to be 22 Gy with a concomitant large decrease in tumor volume, indicating a valid head and neck cancer animal model for radiation studies. Therefore, for further experiments with the HNX-OE tumor line, radiotherapy with a dose of 22 Gy was favored.

To study response monitoring in the HNX-OE xenograft model, a protocol was designed mimicking conventional clinical radiotherapy protocols, with the view of predicting effects of radiotherapy as soon as possible. From FDG studies, it is known that, in general, changes in FDG signal appear before changes can be detected in tumor volume [34]. For FLT, however, little is known. Based on the radiosensitivity experiments, it was assumed that fractionated radiotherapy with a total dose of 22 Gy would result in an adequate radiation dose for determination of the time course of FDG and FLT signals after radiotherapy under conditions that are relevant clinically. Indeed, a significant reduction in tumor volume was observed after this treatment. Tumor growth curves in both FDG and FLT groups

Table 4. Immunohistochemical results in HNX-OE tumor xenografts treated with radiotherapy as compared to control tumors

Group ^a	VEGF	Glut-1	HK I	HK II	HK III	Ki-67 (%)	TK-1	Tumor (%)	Necrosis (%)
FLT	↔	↑	↔	↑	↔	↑	↔	↔	↔
FDG	↔	↑	↔	↑	↔	↑	↔	↔	↔

VEGF Vascular endothelial growth factor, Glut-1 glucose transporter protein-1, HK hexokinase, Ki-67 proliferation marker, TK-1 thymidine kinase 1, Tumor (%) percentage of tumor cells, Necrosis (%) percentage of necrosis, ↔ same range as control; ↑ higher than control

^aMice from the control, FDG, and FLT group were killed, and all tumors were rapidly excised on days 16, 38, and 36, respectively

followed a similar pattern over time. FLT uptake was, however, higher than that of FDG, and both FDG and FLT uptake showed rapid response to radiotherapy. The decrease in FLT uptake as seen in the first week was followed by a much larger decrease in the second week, which was not the case for FDG uptake. For FDG as well as for FLT, a significant decline in retention (relative T/NT ratio) was observed at scan 2 (day 4). Next to this observation, for FLT, the most significant decline in retention (relative T/NT ratio) was observed at scan 4 (day 12); whereas for FDG, this was already noted from scan 2 (day 4). Statistical significance disappeared with respect to scan 4 possibly because of the 4-day period between the last radiotherapy and scan 4. In a study of Sugiyama et al. [35], C₃H/He mice, bearing SCCVII tumors (murine SCC), who received a single dose of 20 Gy, showed a rapid response to radiotherapy both with respect to FDG and FLT uptake in line with the present results.

Several patient studies have demonstrated a significant higher uptake of FDG than FLT in various cancer types [20, 36, 37]. In the present animal model, FDG accumulation in HNX-OE tumor xenografts was relatively low compared to similar animal studies of Zhuang et al. [11] and Dearling et al. [38]. On the other hand, Humm et al. [39] reported that FDG uptake in xenografts grown in rodents was usually low, as most activity was observed in other tissues such as bladder, liver, brain, and heart. Considerable variability in FDG and FLT uptake was observed both before and after radiotherapy. Differences in tumor architecture, like capillary and tumor density and hypoxic and necrotic cell fractions, might have contributed to this variability. In addition, differences in response to radiotherapy might have led to a variance in tracer uptake. Differences in inflammatory reactions, which are conceivable, may alter FDG uptake [5, 8–11]. However, no differences with respect to biomarkers, possibly involved in tracer uptake, were seen between FDG and FLT groups. Compared to the control group, high levels—though not statistically significant—of glucose transporter-1, HK II, and Ki67 expression were found at the end of treatment in both FDG and FLT groups. This might possibly implicate survival of cells with a more aggressive phenotype after treatment. One has to bear in mind, however, that control tumors in this study were excised 16 days after start of the experiments—as a result of tumor load—compared to 36/38 days for the FDG and FLT groups.

With respect to FLT variability, irradiation effects on TK-1 activity have been thought to alter FLT uptake [18, 40]. Temporary inhibition of this key enzyme after low dose irradiation has been reported [41]. In a study of Wei et al. [40], an increase in TK-1 activity was found 24 h after irradiation. Therefore, the time between irradiation and PET scan should be as long as possible to allow for recovery of TK-1 from short-term irradiation effects. A period of 48–72 h between radiotherapy and PET scans used in the present study is, however, considered to be long enough to exclude effects on TK-1.

Humm et al. [39] examined FDG uptake after radiotherapy in rats and found no predictive effect. However, very large variations were observed in starting size of the tumors as well as in tumor growth patterns. Nonetheless, their data did demonstrate a trend between decreasing total FDG accumulation and decreasing tumor burden with an increase in recurrences. In our study, to exclude differences in the initial situation for both tracer groups and to analyze a possible predictive tool, the relationship between tracer uptake and baseline tumor volume was analyzed. A predictive effect by PET tracer uptake on tumor volume after radiotherapy has been found in the presented study: tracer uptake—expressed as baseline T/NT value—predicted tumor volume later on (high baseline uptake predicted small tumors at day 29 [day of tumor regrowth]). A predictive effect of baseline tumor volume itself was not found.

In conclusion, results from this new experimental *in vivo* model support the promise of using FLT-PET, as with FDG-PET, to monitor response to external radiotherapy. This warrants further clinical studies to compare these two tracers especially in cancers treated with radiotherapy.

Acknowledgment. We thank the expert assistance of Marijke Stigter-van Walsum for implantation of the head and neck xenografts, Pieter Klein and Martien Mooijer for synthesizing FLT, and Fred Buijs, Hugo de Jong, and Reina Kloet for help in operating the HRRT PET scanner. Stan Heukelom is acknowledged for help in radiation dose calculations, Gerrit Meijer and Marc Broeckaert for help in (immuno)histological examinations, and Ronald Boellaard for help with T/NT analysis.

References

1. Lowe VL, SJB (2003) PET imaging head and neck cancer. In: Valk PE, Bailey DL, Townsend DW, Maisey MN (eds) Positron emission tomography. London: Springer
2. Kim MM, Califano JA (2004) Molecular pathology of head-and-neck cancer. *Int J Cancer* 112:545–553
3. Schwartz DL, Rajendran J, Yueh B, et al. (2004) FDG-PET prediction of head and neck squamous cell cancer outcomes. *Arch Otolaryngol Head Neck Surg* 130:1361–1367
4. Hardisson D (2003) Molecular pathogenesis of head and neck squamous cell carcinoma. *Eur Arch Otorhinolaryngol* 260:502–508
5. Klabbers BM, Lammertsma AA, Slotman BJ (2003) The value of positron emission tomography for monitoring response to radiotherapy in head and neck cancer. *Mol Imag Biol* 5:257–270
6. Pauwels EK, Sturm EJ, Bombardieri E, Cleton FJ, Stokkel MP (2000) Positron-emission tomography with [18F]fluorodeoxyglucose. Part I. Biochemical uptake mechanism and its implication for clinical studies. *J Cancer Res Clin Oncol* 126:549–559
7. Maschauer S, Prante O, Hoffmann M, Deichen JT, Kuwert T (2004) Characterization of 18F-FDG uptake in human endothelial cells *in vitro*. *J Nucl Med* 45(3):455–460
8. Brun E, Ohlsson T, Erlandsson K, et al. (1997) Early prediction of treatment outcome in head and neck cancer with 2-18FDG PET. *Acta Oncol* 36(7):741–747
9. Hautzel H, Muller-Gartner HW (1997) Early changes in fluorine-18-FDG uptake during radiotherapy. *J Nucl Med* 38:1384–1386
10. Kubota R, Yamada S, Kubota K, Ishiwata K, Tamahashi N, Ido T (1992) Intratumoral distribution of fluorine-18-fluorodeoxyglucose *in vivo*: high accumulation in macrophages and granulation tissues studied by microautoradiography. *J Nucl Med* 33:1972–1980
11. Zhuang H, Pourdehnad M, Lambright ES, et al. (2001) Dual time point 18F-FDG PET imaging for differentiating malignant from inflammatory processes. *J Nucl Med* 42:1412–1417
12. Direcks WGE, Lammertsma AA, Molthoff CF (2006) 3'-Deoxy-3'-18F-Fluorothymidine as a tracer of proliferation in positron emission tomography. In: GJ Peters (ed) Cancer drug discovery and development,

- deoxynucleoside analogs in cancer therapy. Totowa, NJ, USA: Humana Press Inc., pp 441–462
13. Shields AF, Grierson JR, Dohmen BM, et al. (1998) Imaging proliferation *in vivo* with [F-18]FLT and positron emission tomography. *Nat Med* 4:1334–1336
 14. Vesselle H, Grierson J, Muzi M, et al. (2002) *in vivo* validation of 3'-deoxy-3'-[(18)F]fluorothymidine ([F-18]FLT) as a proliferation imaging tracer in humans: correlation of [F-18]FLT uptake by positron emission tomography with Ki-67 immunohistochemistry and flow cytometry in human lung tumors. *Clin Cancer Res* 8: 3315–3323
 15. Arner ES, Eriksson S (1995) Mammalian deoxyribonucleoside kinases. *Pharmacol Ther* 67:155–186
 16. Barthel H, Perumal M, Latigo J, et al. (2005) The uptake of 3'-deoxy-3'-[F-18]fluorothymidine into L5178Y tumours *in vivo* is dependent on thymidine kinase 1 protein levels. *Eur J Nucl Med Mol Imaging* 32:257–263
 17. Grierson JR, Schwartz JL, Muzi M, Jordan R, Krohn KA (2004) Metabolism of 3'-deoxy-3'-[F-18]fluorothymidine in proliferating A549 cells: validations for positron emission tomography. *Nucl Med Biol* 31:829–837
 18. Rasey JS, Grierson JR, Wiens LW, Kolb PD, Schwartz JL (2002) Validation of FLT uptake as a measure of thymidine kinase-1 activity in A549 carcinoma cells. *J Nucl Med* 43:1210–1217
 19. Shields AF (2003) PET imaging with 18F-FLT and thymidine analogs: promise and pitfalls. *J Nucl Med* 44:1432–1434
 20. van Westreenen HL, Cobben DC, Jager PL, et al. (2005) Comparison of 18F-FLT PET and 18F-FDG PET in esophageal cancer. *J Nucl Med* 46:400–404
 21. van Waarde A, Cobben DC, Suurmeijer AJ, et al. (2004) Selectivity of 18F-FLT and 18F-FDG for differentiating tumor from inflammation in a rodent model. *J Nucl Med* 45(4):695–700
 22. Klaassen I, Brakenhoff RH, Smeets SJ, Snow GB, Braakhuis BJ (2001) Expression of retinoic acid receptor gamma correlates with retinoic acid sensitivity and metabolism in head and neck squamous cell carcinoma cell lines. *Int J Cancer* 92:661–665
 23. Welters MJ, Fichtinger-Schepman AM, Baan RA, et al. (1997) Relationship between the parameters cellular differentiation, doubling time and platinum accumulation and cisplatin sensitivity in a panel of head and neck cancer cell lines. *Int J Cancer* 71:410–415
 24. Molthoff CF, Calame JJ, Pinedo HM, Boven E (1991) Human ovarian cancer xenografts in nude mice: characterization and analysis of antigen expression. *Int J Cancer* 47:72–79
 25. Peters GJ, Van Dijk J, Nadal JC, Van Groeningen CJ, Lankelma J, Pinedo HM (1987) Diurnal variation in the therapeutic efficacy of 5-fluorouracil against murine colon cancer. *in vivo* 1:113–117
 26. Tomayko MM, Reynolds CP (1989) Determination of subcutaneous tumor size in athymic (nude) mice. *Cancer Chemother Pharmacol* 24: 148–154
 27. Machulla HJ, Blocher A, Kuntzsch M, Piert M, Wei R, Grierson JR (2000) Simplified labeling approach for synthesizing 3'-deoxy-3'-[F-18]fluorothymidine ([F-18]FLT). *J Radioanal Nucl Chem* 243: 843–846
 28. de Jong H, Knoess C, Lammertsma AA, et al. (2004) Performance characteristics of the high resolution research tomograph comparison of three prototypes. *IEEE Med Imaging Conf Record* 6:3437–3439
 29. van der Veldt AA, Hooft L, van Diest PJ, et al. (2006) Microvessel density and p53 in detecting cervical cancer by FDG PET in cases of suspected recurrence. *Eur J Nucl Med Mol Imaging* 33:1408–1416
 30. Bos R, van der Hoeven JJM, van der Wall E, et al. (2002) Biologic correlates of 18Fluorodeoxyglucose uptake in human breast cancer measured by positron emission tomography. *J Clin Oncol* 20: 379–387
 31. Hooft L, van der Veldt AA, van Diest PJ, et al. (2005) [18F]fluorodeoxyglucose uptake in recurrent thyroid cancer is related to hexokinase i expression in the primary tumor. *J Clin Endocrinol Metab* 90:328–334
 32. Milas L, Mason K, Hunter N, et al. (2000) *in vivo* enhancement of tumor radioresponse by C225 antiepidermal growth factor receptor antibody. *Clin Cancer Res* 6:701–708
 33. Jackel MC, Kopf-Maier P, Baumgart F, Ziessow D, Tausch-Tremel R (2000) Value of 31P NMR spectroscopy in predicting the response of a xenografted human hypopharynx carcinoma to irradiation. *J Cancer Res Clin Oncol* 126:325–331
 34. Kostakoglu L, Goldsmith SJ (2003) 18F-FDG PET evaluation of the response to therapy for lymphoma and for breast, lung, and colorectal carcinoma. *J Nucl Med* 44:224–239
 35. Sugiyama M, Sakahara H, Sato K, et al. (2004) Evaluation of 3'-deoxy-3'-18F-fluorothymidine for monitoring tumor response to radiotherapy and photodynamic therapy in mice. *J Nucl Med* 45:1754–1758
 36. Cobben DC, van der Laan BF, Maas B, et al. (2004) 18F-FLT PET for visualization of laryngeal cancer: comparison with 18F-FDG PET. *J Nucl Med* 45:226–231
 37. Smyczek-Gargya B, Fersis N, Dittmann H, et al. (2004) PET with [18F]fluorothymidine for imaging of primary breast cancer: a pilot study. *Eur J Nucl Med Mol Imaging* 31:720–724
 38. Dearing JL, Flynn AA, Sutcliffe-Goulden J, et al. (2004) Analysis of the regional uptake of radiolabeled deoxyglucose analogs in human tumor xenografts. *J Nucl Med* 45:101–107
 39. Humm JL, Lee J, O'Donoghue JA, et al. (1999) Changes in FDG tumor uptake during and after fractionated radiation therapy in a rodent tumor xenograft. *Clin Positron Imaging* 2:289–296
 40. Wei S, Ageron-Blanc A, Petridis F, Beaumatin J, Bonnet S, Luccioni C (1999) Radiation-induced changes in nucleotide metabolism of two colon cancer cell lines with different radiosensitivities. *Int J Radiat Biol* 75:1005–1013
 41. Hohn-Elkarim K, Muhlensiepen H, Altman KI, Feinendegen LE (1990) Modification of effects of radiation on thymidine kinase. *Int J Radiat Biol* 58:97–110